# Elongated Thrombin Binding Aptamer: A G-Quadruplex Cation-Sensitive Conformational Switch

**ARTICLE** *in* CHEMISTRY - A EUROPEAN JOURNAL · FEBRUARY 2012

Impact Factor: 5.73 · DOI: 10.1002/chem.201103381 · Source: PubMed



**4 AUTHORS:**

Aurore De Rache
Institut Européen De Chimie Et Biologie
**13** PUBLICATIONS **64** CITATIONS
SEE PROFILE

Iva Kejnovska
Institute of Biophysics ASCR
**37** PUBLICATIONS **1,001** CITATIONS
SEE PROFILE

Michaela Vorlickova
Masaryk University
**127** PUBLICATIONS **2,418** CITATIONS
SEE PROFILE

Claudine Buess-Herman
Université Libre de Bruxelles
**86** PUBLICATIONS **1,355** CITATIONS
SEE PROFILE

CHEMISTRY
A EUROPEAN JOURNAL

DOI: 10.1002/chem.201103381

# Elongated Thrombin Binding Aptamer: A G-Quadruplex Cation-Sensitive Conformational Switch

**Aurore De Rache,[a] Iva Kejnovská,[b] Michaela Vorlíčková,[b] and Claudine Buess-Herman*[a]**

**Abstract:** Aptamer-based biosensors offer promising perspectives for high performance, specific detection of proteins. The thrombin binding aptamer (TBA) is a G-quadruplex-forming DNA sequence, which is frequently elongated at one end to increase its analytical performances in a biosensor configuration. Herein, we investigate how the elongation of TBA at its 5′ end affects its structure and stability. Circular dichroism spectroscopy shows that TBA folds in an antiparallel G-quadruplex conformation with all studied cations ($Ba^{2+}$, $Ca^{2+}$, $K^+$, $Mg^{2+}$, $Na^+$, $NH_4^+$, $Sr^{2+}$ and the $[Ru(NH_3)_6]^{2+/3+}$ redox marker) whereas other structures are adopted by the elongated aptamers in the presence of some of these cations. The stability of each structure is evaluated on the basis of UV spectroscopy melting curves. Thermal difference spectra confirm the quadruplex character of all conformations. The elongated sequences can adopt a parallel or an antiparallel structure, depending on the nature of the cation; this can potentially confer an ion-sensitive switch behavior. This switch property is demonstrated with the frequently employed redox complex $[Ru(NH_3)_6]^{3+}$, which induces the parallel conformation at very low concentrations (10 equiv per strand). The addition of large amounts of $K^+$ reverts the conformation to the antiparallel form, and opens interesting perspectives for electrochemical biosensing or redox-active responsive devices.

**Keywords:** circular dichroism · DNA structures · G-quadruplexes · hexa-ammine ruthenium · thermal difference spectra

## Introduction

Since the elaboration of the SELEX method (systematic evolution of ligands by exponential enrichment) to isolate first RNA[1] and subsequently DNA[2] sequences with a high affinity for a target, the so-selected sequences, called aptamers, have been intensively used. As aptamers are nucleic acid sequences selected in vitro, they can be designed against a wider variety of targets than antibodies. Together with the possibility to select aptamers stable in extreme conditions, this selection method provides a large field of applications for aptamers and makes them promising probes for sensing.[3]

Thrombin was the first protein against which a DNA aptamer was selected[2] and characterized.[4] Because thrombin is a commercially available protein and DNA is easier to handle than RNA, a variety of techniques like fluorescence,[5] SPR,[6] QCM,[7] AFM,[8] electrogenerated chemiluminescence[9] or electrochemistry[7b,c,10] have been employed to demonstrate the possible detection of this protein target by using its DNA aptamer probe.

In order to achieve efficient transduction, many methods require the immobilization of the probe on a surface. For such methods, it has been shown[6b] that conferring some flexibility to the probe by moving it slightly away from the surface increases the accessibility for the target and enhances the analytical performance. Therefore, many studies use a probe that is both chemically modified, to achieve its anchoring to the surface (usually by a thiol group or a biotin)[11] and lengthened by the addition of a few nucleotides that are not involved in the recognition event.[6a,b,d,7a,c,8,10a–c]

The thrombin binding aptamer (TBA) has the antiparallel quadruplex forming sequence GGTTGGTGTGGTTGG.[4a,b,f] Quadruplex structures play essential roles in molecular biology. In particular, telomeres are responsible for regulation of cellular senescence, and their elongation by telomerase is related to cancer.[12] It has been shown that the structure of telomeres is very sensitive to nucleotide addition at the 5′ end.[13] TBA is a quadruplex-forming sequence and is susceptible to adopt a different folding, when it is modified, and particularly when it is elongated. Modifications made within the 15-mer core sequence of TBA identified as the recognition pattern against thrombin have already been studied thoroughly.[14] On the contrary, the influence of the addition of a few nucleotides at one

[a] A. De Rache, Prof. C. Buess-Herman
Université Libre de Bruxelles, Faculté des Sciences
Service de Chimie Analytique et Chimie des Interfaces, CP 255
Boulevard du Triomphe 2, 1050 Bruxelles (Belgium)
Fax: (+32) 2-650-29-34
E-mail: cbuess@ulb.ac.be

[b] Dr. I. Kejnovská, Prof. M. Vorlíčková
Institute of Biophysics
Academy of Sciences of the Czech Republic v.v.i.
Královopolská 135, 612 65 Brno (Czech Republic)

Supporting information for this article is available on the WWW under http://dx.doi.org/10.1002/chem.201103381.

end of the sequence of the aptamer structure, has been so far scarcely investigated: one study was devoted to the influence of different numbers of thymines added to the probe on thrombin detection,[6b] but no structural information was provided, and another study was limited to potassium medium.[4a] In this work, we investigate how the structure of TBA can be affected by the incorporation of two different sets of six nucleotides at the 5′ end, chosen on the basis of studies reported earlier;[4a,6b] Table 1 gives the studied sequences.

Table 1. Studied oligonucleotides.

| Sequence | $\varepsilon$ at 260 nm [$M^{-1}cm^{-1}$] | Name |
|---|---|---|
| 5′-GGTTGGTGTGGTTGG-3′ | 143300 | TBA |
| 5′-TTTTTTGGTTGGTGTGGTTGG-3′ | 191300 | TTTTTT-TBA |
| 5′-GTAGGTGGTTGGTGTGGTTGG-3′ | 205000 | GTAGGT-TBA |

The folding and stability of G-quadruplexes are particularly sensitive to cations.[4b,15] This property has led some groups to propose the use of quadruplexes as a metal detection platform,[16] "DNA logic gates",[17] and molecular switches for charge transport,[18] intramolecular energy transfer[19] or binding affinity.[20] Besides such materials-driven applications, establishing the structure and stability of aptamers in the presence of different cations is essential from the biosensing perspective, since any change in the structure of the aptamer could influence its sensing capacity. Some cations like $[Ru(NH_3)_6]^{3+}$ are used in detection methods for their electrochemical properties. Steel et al.[21] developed a method to determine the DNA probe surface coverage by a simple electrochemical measurement relying on the electrostatic interactions between the negatively charged phosphate groups of DNA and the positively charged redox marker $[Ru(NH_3)_6]^{3+}$ present in the electrolyte. Steel's method—nowadays widespread—is based on the assumption of perfect charge compensation between the phosphate groups and the marker. Nevertheless, any specific folding of the DNA could reduce the accessibility of the redox marker to the probe. Furthermore, the presence of the redox marker in solution can influence the folding of DNA as various cations can stabilize different DNA structures,[15a,22] and complex cations like $[Co(NH_3)_6]^{3+}$ and $[Ru(NH_3)_6]^{3+}$ are known to induce conformational changes, such as the B→Z duplex transition.[23] Particular attention is thus devoted in this work to the $[Ru(NH_3)_6]^{2+/3+}$ redox marker and how its interaction with DNA aptamers influences their folding. For this purpose, structural investigations of two different lengthened sequences are performed by CD and UV absorption spectroscopy in the presence of various cations including the hexa-ammineruthenium complexes. The stability of the observed structures is checked by thermal denaturation and in some cases the occurrence of quadruplex arrangement is confirmed by thermal difference absorption spectra (TDS). The TBA sequence is used as a reference system throughout the present work.

## Results and Discussion

**CD spectroscopy**: The TBA sequence has been already extensively studied and its CD spectrum in the presence of $K^+$ is well-established. Therefore, we started by comparing the CD spectra obtained in $K^+$-containing solutions for TBA with those recorded for the elongated TBA sequences. As shown in Figure 1, the CD spectra of the three sequences

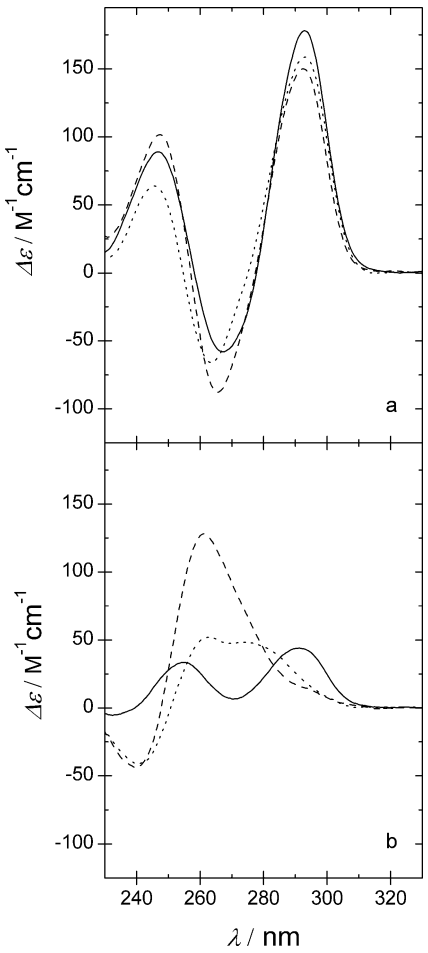


Figure 1. CD spectra in Tris buffer (pH 7.4) in the presence of: a) 25 mM KCl, b) 10 equiv $[Ru(NH_3)_6]^{3+}$ per DNA strand; TBA (——), GTAGGT-TBA (-----), and TTTTTT-TBA (•••••). (A color version of this Figure can be found in the Supporting Information.)

present similar characteristics in the presence of potassium ions: two maxima located at 246–247 nm and 293 nm and one minimum at 267, 266 and 264 nm for TBA, GTAGGT-TBA and TTTTTT-TBA, respectively. These peaks are characteristic of an antiparallel quadruplex structure[22] and confirm earlier data obtained for TBA[4a,b,f,g] and GTAGGT-TBA.[4a]

In contrast to this similar behavior observed for the three sequences in the presence of potassium ions, CD spectra obtained in the presence of hexa-ammineruthenium(III) complex (Figure 1b) present various morphologies depending on the sequence. The large difference in the shape of CD

  

spectra motivated us to study these sequences in the presence of non-complex cations, namely $Na^+$, $K^+$, $Rb^+$, $NH_4^+$, $Mg^{2+}$, $Ca^{2+}$, $Sr^{2+}$ and $Ba^{2+}$, to obtain a better insight for the analysis.

The CD spectra of the TBA sequence measured in the presence of $Na^+$, $K^+$, $Rb^+$, $NH_4^+$, $Mg^{2+}$ or $Ca^{2+}$ present two positive bands at around 245 and 290 nm interconnected with a negative band at about 270 nm (Figure 2a). The

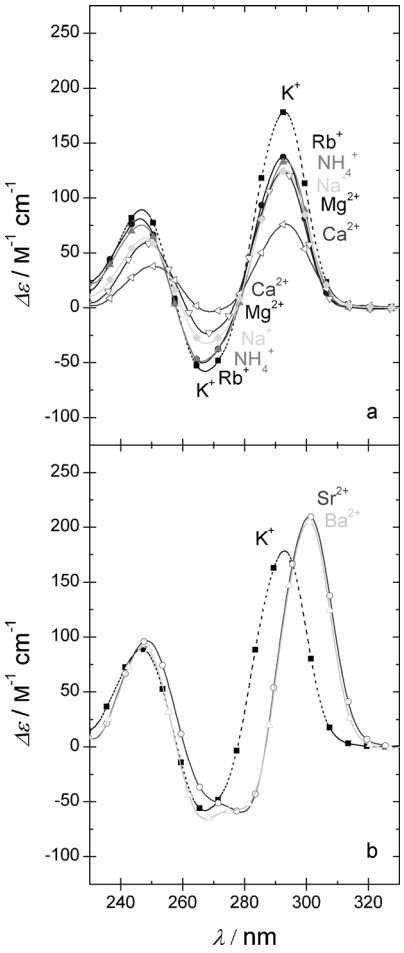


Figure 2. CD spectra of TBA measured in Tris buffer (pH 7.4) in the presence of: a) $Ca^{2+}$, $K^+$, $Mg^{2+}$, $Na^+$, $NH_4^+$ and $Rb^+$, and b) $Ba^{2+}$ and $Sr^{2+}$ (the CD spectrum measured with $K^+$ is plotted for easier comparison). The concentrations of monovalent and divalent ions were 25 and 5 mM, respectively. (A color version of this Figure can be found in the Supporting Information.)

shape of the CD spectra shows that the same type of structure is formed with all these ions. The different magnitudes of the bands can reflect various extents of structure arrangement. These observations evidence the formation of an antiparallel quadruplex structure and are consistent with a previous cation-dependence study performed on this sequence.[4b] In the presence of $Sr^{2+}$ or $Ba^{2+}$ the CD spectra show a significant shift in the second positive peak to higher wavelengths (Figure 2b), in agreement with the aforementioned study.[4b] An NMR spectroscopy study[24] performed in $Sr^{2+}$ solutions has shown that the structure formed in this case is still an antiparallel quadruplex, but with an intertetrad distance of 3.8 Å, which is 0.7 Å longer than that formed with potassium ions.

Regardless of the cation present in solution, TBA always folds into an antiparallel quadruplex. Although the two lengthened DNA strands contain the same quadruplex-forming sequence as TBA, they do not behave identically in the presence of all cations. The characteristic antiparallel fingerprint pictured for TBA in Figure 2a is obtained only with $K^+$ and $Rb^+$ for GTAGGT-TBA (Figure 3a) and with $K^+$, $Rb^+$ and $NH_4^+$ for TTTTTT-TBA (Figure 3b). The shift of the second positive peak is observed for $Ba^{2+}$ and $Sr^{2+}$ with both sequences, as in the case of TBA.

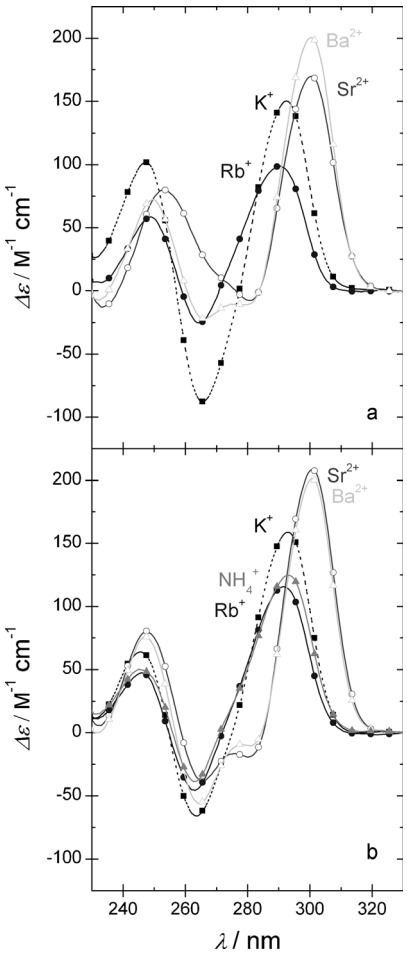


Figure 3. CD spectra of: a) GTAGGT-TBA, and b) TTTTTT-TBA in Tris buffer (pH 7.4) in the presence of different ions inducing antiparallel quadruplex structure: concentrations of monovalent and divalent ions were 25 and 5 mM, respectively. (A color version of this Figure can be found in the Supporting Information.)

Although similar topologies were observed for TBA and the two lengthened sequences in the presence of certain cations, other ions led to markedly different behaviors. Figure 4a presents the CD spectra in $Na^+$-, $Mg^{2+}$- or $Ca^{2+}$-containing solutions for the GTAGGT-TBA sequence. They ex-

  

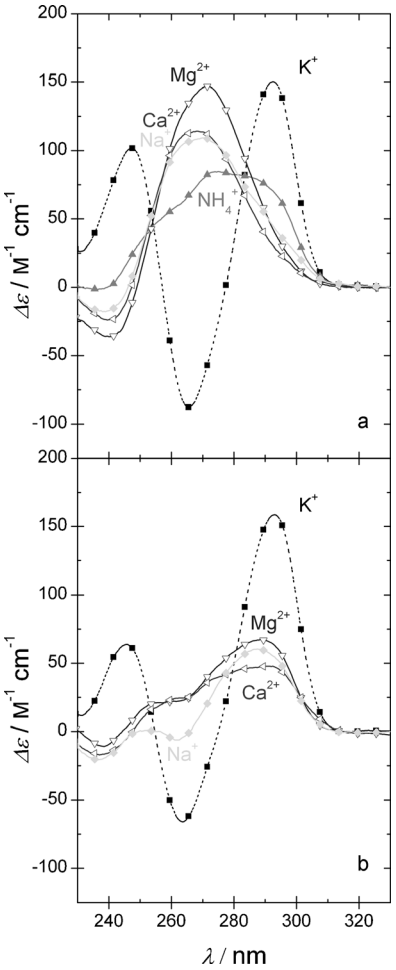


Figure 4. CD spectra of: a) GTAGGT-TBA, and b) TTTTTT-TBA in Tris buffer (pH 7.4) in the presence of different ions inducing parallel or mixed quadruplex structures (except with $K^+$, plotted for comparison); concentrations of monovalent and divalent ions were 25 and 5 mM, respectively. (A color version of this Figure can be found in the Supporting Information.)

hibit a negative band at around 240 nm and a positive band, the position of which varies between 265 and 275 nm (Figure 4a).

These characteristics are reminiscent of a parallel quadruplex structure,[25] though the observed positive peak is smaller than the usual shape for this type of structure. The spectrum of GTAGGT-TBA in $NH_4^+$ is rather ill-defined, and presents only a broad positive contribution between 250 and 300 nm, so that no clear type of quadruplex structure can be proposed on the sole basis of CD spectroscopy.

When TTTTTT-TBA is in a solution containing $Na^+$, $Ca^{2+}$ or $Mg^{2+}$ (Figure 4b), the pronounced decrease of the intensity of the peak at around 290 nm indicates that the antiparallel quadruplex is destabilized. The presence of a slightly negative band at around 240 nm and the disappearance of the negative band at about 260 nm seem more indicative of a parallel quadruplex. Therefore, we suggest that the spectra reflect a mixture of parallel and antiparallel arrangements.

**UV absorption (thermal stability)**: To confirm whether or not the sequences adopt quadruplex topologies with these cations, we performed additional analyses by UV absorption spectroscopy. Mergny et al.[26] noted that the quadruplex formation can be followed by hyperchromism (increase of absorbance) in the long wavelength part of UV absorption spectra. Because the largest hyperchromism is observed at 295 nm, this wavelength is used to study the thermal denaturation of quadruplex structures. Figure 5 shows the tempera-

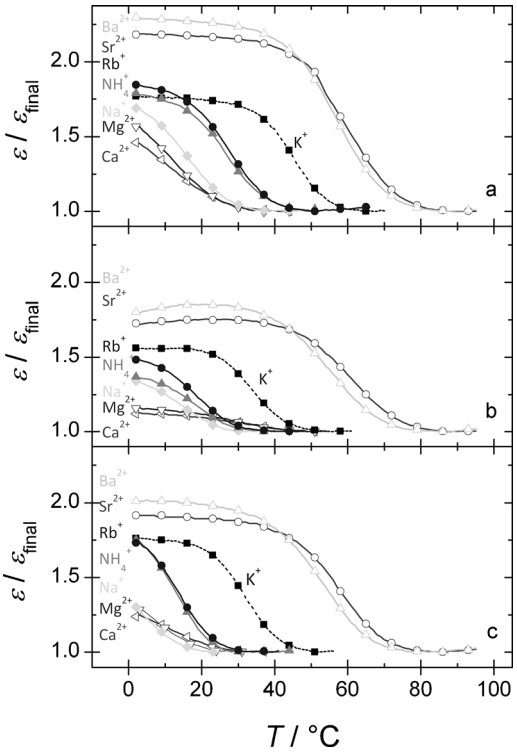


Figure 5. Temperature dependence of the normalized absorbance at 295 nm (see main text for details) of: a) TBA, b) GTAGGT-TBA, and c) TTTTTT-TBA in Tris buffer in the presence of different cations; concentration of monovalent and divalent ions were 25 and 5 mM, respectively. (A color version of this Figure can be found in the Supporting Information.)

ture dependences of the absorbance at 295 nm for TBA, GTAGGT-TBA and TTTTTT-TBA, in the presence of all studied cations.

For the TBA sequence (Figure 5a), one can observe a cooperative decrease of the absorbance at 295 nm with all ions. The relative thermal stability in the presence of the different cations can be estimated by their melting temperature, $T_m$. These $T_m$ values were determined by the median method, as recommended by Mergny and Lacroix[27] and are reported in Table 2.

The stability of the TBA structure decreases according to the cation sequence $Sr^{2+} \approx Ba^{2+} > K^+ > Rb^+ \approx NH_4^+ > Na^+$, in agreement with the literature.[4b] The $T_m$ values for $Ca^{2+}$ and $Mg^{2+}$ could not be determined because their thermal denaturation seems to have already begun at the lowest temperature, 2 °C. With GTAGGT-TBA and TTTTTT-TBA

  

Table 2. Melting temperature of the structures formed in the presence of various cations.

| Cation | TBA [°C] | GTAGGT-TBA [°C] | TTTTTT-TBA [°C] |
|---|---|---|---|
| $Sr^{2+}$ | 60 | 60 | 57 |
| $Ba^{2+}$ | 57 | 55 | 52 |
| $K^+$ | 45 | 35 | 33 |
| $Rb^+$ | 29 | 18 | 15 |
| $NH_4^+$ | 28 | 20 | 14 |
| $Na^+$ | 16[a] | 15[a] | _[b] |
| $Ca^{2+}$ | _[b] | _[b] | _[b] |
| $Mg^{2+}$ | _[b] | _[b] | _[b] |

[a] Values could be overestimated due to the possible start of the denaturation process before 2 °C. [b] Value could not be determined.

(Figure 5b and c, respectively) the decrease in the absorbance measured at 295 nm is observed for all ions. In the case of GTAGGT-TBA, all cations led to smaller $T_m$ than for TBA, except $Sr^{2+}$, which presents the same $T_m$ value (Table 2). For TTTTTT-TBA, $T_m$ values (Table 2) are systematically smaller than for TBA and generally lower in comparison with GTAGGT-TBA. This point is particularly important for applications that use lengthened TBA as it could influence the available working range of the aptamer. It should be mentioned that for the three sequences and all the cations studied, the denaturation was reversible and no hysteresis was observed between denaturation (increasing temperature) and renaturation (decreasing temperature) curves (see the Supporting Information). This indicates that the structures undergoing denaturation are probably intramolecular, in contrast to multiple stranded structures, which display hysteresis.[27,28]

**Thermal difference spectra**: The presence of a hypochromic shift at 295 nm is a strong, though non-specific indication of the formation of quadruplexes. The UV absorption data can be further analyzed in terms of thermal difference spectra, the shapes of which are specific for the adopted conformation.[29] The TDS of the three sequences are presented in Figure 6. The spectra obtained for TBA (Figure 6a), the antiparallel quadruplex structure of which is established, can be used as reference for the interpretation of the TDS data obtained for the elongated sequences. With most cations, the curves show two maxima at around 242 and 273 nm and two minima at about 262 and 295 nm, in agreement with the literature on TBA.[29,30] The spectra obtained with the lengthened sequences are similar to those of TBA (Figure 6b and c), and display the same characteristics for all cations. A comparison with the curves reported in the literature[29] reveals that the shape of the curves is compatible only with a quadruplex structure. A more detailed description, interpretation and comparison of the TDS is provided in the Supporting Information.

The results from thermal difference spectra definitely confirm the quadruplex character of all observed structures. It is now possible to analyses the CD spectra of GTAGGT-TBA (Figure 4a) in the presence of $NH_4^+$ and of TTTTTT-TBA in $Na^+$, $Ca^{2+}$ and $Mg^{2+}$ (Figure 4b) solutions, and

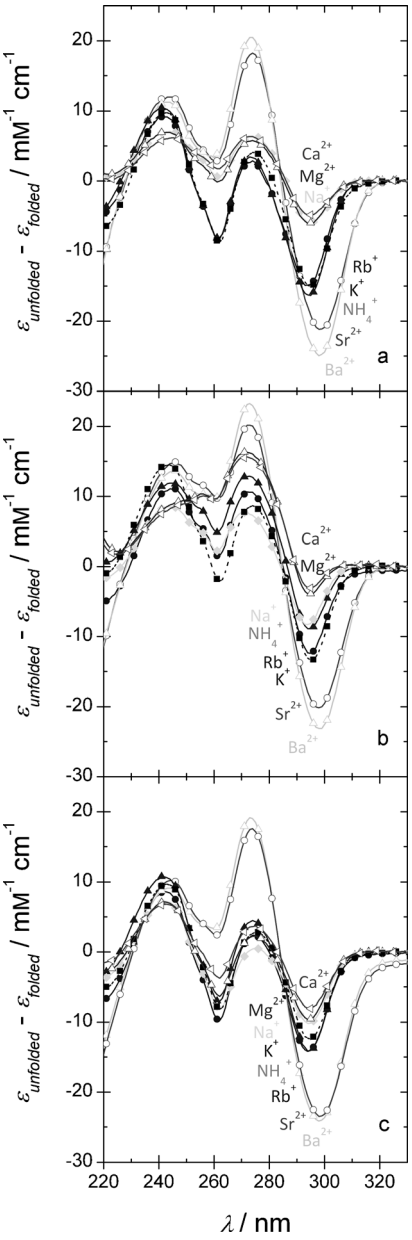


Figure 6. TDS spectra of: a) TBA, b) GTAGTT-TBA, and c) TTTTTT-TBA in Tris buffer (pH 7.4) in the presence of different cations; concentration of monovalent and divalent cations were 25 and 5 mM, respectively. (A color version of this Figure can be found in the Supporting Information.)

they can presumably be assigned to mixtures of parallel and antiparallel quadruplexes. On the same grounds the CD spectra of GTAGGT-TBA in the presence of $Na^+$, $Ca^{2+}$ and $Mg^{2+}$ can be attributed to parallel quadruplex structures with low stability.

**Quadruplexes in the presence of $[Ru(NH_3)_6]^{2+/3+}$ complexes (CD spectra)**: Our systematic study of the three DNA sequences in the presence of various cations has shown that different structures can be observed depending both on the nature of the cation and on the sequence of nucleotides

  

chosen to elongate the TBA sequence. Therefore, the differences observed in Figure 1b between the CD spectra of the three sequences in the presence of $[Ru(NH_3)_6]^{3+}$ cannot be directly connected with the complex nature of this ion but to the elongated TBA sequence.

In order to assess the influence of this hexa-ammineruthenium redox marker, we have also examined the characteristics of the structures adopted in the presence of its reduced form, $[Ru(NH_3)_6]^{2+}$. Figure 7 presents the CD spectra recorded at various temperatures for TBA, GTAGGT-TBA and TTTTTT-TBA in the presence of $[Ru(NH_3)_6]^{2+}$. Focusing first on the spectra recorded at 5°C (solid lines), it can be seen that the curves are very similar to those obtained in the presence of $[Ru(NH_3)_6]^{3+}$ (Figure 1b), under otherwise identical conditions.

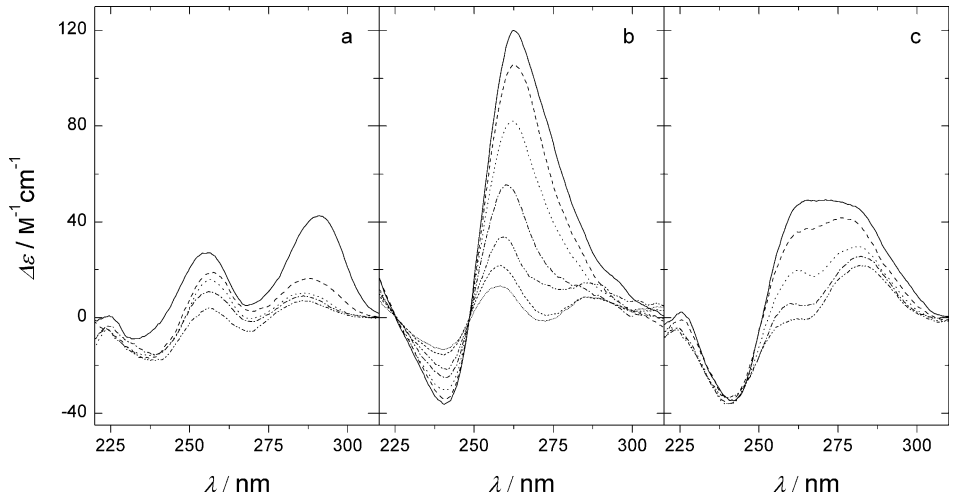


Figure 7. Thermal denaturation of the structures formed in the presence of $[Ru(NH_3)_6]^{2+}$. CD spectra of: a) TBA, b) GTAGTT-TBA, and c) TTTTTT-TBA in Tris buffer (pH 7.4) in the presence of 10 equiv $[Ru(NH_3)_6]^{2+}$ measured every 10°C starting from 5°C (solid line).

In the case of TBA one can observe two positive bands at around 253 and 290 nm interconnected by a depression at about 270 nm (Figure 7a). The spectrum is rather similar to the spectrum recorded in $Ca^{2+}$ solutions (Figure 2a), though with smaller values of $\Delta\varepsilon$. The corresponding structure is an antiparallel quadruplex with a lower stability than the one observed with the divalent calcium ions. In contrast to TBA, the CD spectrum of GTAGGT-TBA exhibits a negative band at 242 nm and an intense positive one at around 264 nm (Figure 7b). According to the similar shapes observed in the presence of hexa-ammineruthenium and $Ca^{2+}$ or $Na^+$ solutions (Figure 4a), a parallel quadruplex is suggested for the folded structure. The spectrum of TTTTTT-TBA has a negative band at around 242 nm and a broad positive band between 260 and 285 nm (Figure 7c). It is reported in the literature that the CD spectrum of successive thymines presents a positive contribution at around 280 nm and a negative one at about 260 nm.[31] The TTTTTT-TBA spectrum could thus correspond to a majority of parallel quadruplex folding.

**Thermal denaturation**: The CD spectra obtained in the presence of $[Ru(NH_3)_6]^{2+}$ at increasing temperatures are presented for TBA, GTAGGT-TBA and TTTTTT-TBA (Figure 7a–c, respectively; broken lines). For the TBA sequence, an important decrease of the positive band at around 290 nm is observed between 5 and 15°C. Further increase in temperature does not lead to any marked change. The thermal denaturation of GTAGGT-TBA induces a cooperative two-state decrease of the positive band at around 264 nm and of the negative band at about 242 nm, up to 65°C. Two isoelliptic points are observed at 225 and 248 nm. For TTTTTT-TBA, a decrease of the positive band centered at around 260 nm is observed whereas no change is noted for the negative contribution at about 242 nm. The decrease of the positive contribution centered at 280 nm is smaller than that at 260 nm. The higher stability of this contribution would agree with its attribution to the terminal thymines[31] and strengthens the hypothesis of a predominant parallel arrangement. With the three sequences, the CD spectra recorded during thermal denaturation in $[Ru(NH_3)_6]^{3+}$ are very similar to those observed in $[Ru(NH_3)_6]^{2+}$; thus, both complexes induce structures of similar stability. A higher stability is obtained for the sequences adopting the parallel folding, especially in the case of GTAGGT-TBA.

**Structural competition**: While TBA folds exclusively in an antiparallel quadruplex, the two lengthened sequences can fold either in a parallel or an antiparallel quadruplex conformation depending on the nature of the cation. Therefore, by choosing proper experimental conditions, it should be possible to observe a conformational transition between the parallel and the antiparallel quadruplex structure of the elongated aptamers. Such conformational change can be induced by ionic competition. Figure 8a shows the effect of ionic competition between $[Ru(NH_3)_6]^{3+}$ and $K^+$ in the case of the GTAGGT-TBA sequence, for which the concentration of $K^+$ was increased gradually.

The starting curve was recorded in the presence of 10 equiv $[Ru(NH_3)_6]^{3+}$ per strand and in the absence of $K^+$ ion. Upon increasing the concentration of $K^+$, the switch from parallel to antiparallel quadruplex is clearly evidenced by the rise of the positive band at around 295 nm, the transformation of the positive contribution at about 260 nm into a negative one, and the concomitant inversion of the contribution at approximately 240 nm. The presence of two isoelliptic points located at 252 and 282 nm confirms a two-state switch between the two. A similar competition effect for the

  

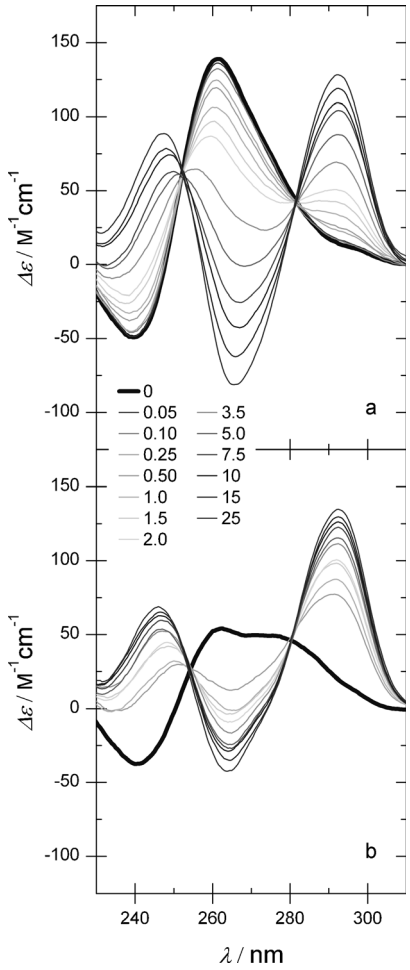


Figure 8. Competition effect between 10 equiv $[Ru(NH_3)_6]^{3+}$ (thick line) and increasing $K^+$ concentrations [mM] in the case of: a) GTAGGT-TBA, and b) TTTTTT-TBA. (A color version of this Figure can be found in the Supporting Information.)

TTTTTT-TBA sequence is presented in Figure 8b, which also presents a two-state transition to an antiparallel quadruplex during the competition between the redox marker and the potassium ions. The comparison between the two sequences clearly shows that the relative stability of the parallel quadruplex is higher in the case of GTAGGT-TBA. Indeed, in the presence of 0.5 mM $K^+$, the GTAGGT-TBA spectrum still exhibits the parallel quadruplex characteristics whereas the TTTTTT-TBA spectrum has already shifted to antiparallel characteristics.

From the above results, such competition effect could be expected with cations other than $[Ru(NH_3)_6]^{3+}$. For instance, mixtures of $K^+$ and $Mg^{2+}$ cations are frequently encountered in biosensing. We have, thus, performed a similar competition experiment between these two cations, the results of which are presented in Figure S4 in the Supporting Information. In this case as well, a transition between the parallel and the antiparallel folding was obtained for both sequences and the conversion of TTTTTT-TBA to a majority of antiparallel quadruplex required smaller $K^+$ concentrations than with the GTAGGT-TBA case.

## Conclusion

In this work, we have studied the influence of the incorporation of two sets of additional nucleotides at the 5′ end of the thrombin binding aptamer on the structure it adopts in the presence of various monovalent or bivalent cations, and of a cationic redox marker. Similar to TBA, the two lengthened sequences fold into an antiparallel quadruplex in $K^+$-containing solutions. The capability of these two elongated sequences to adopt this conformation, which is necessary to the interaction between thrombin and its aptamer, is maintained upon lengthening; their use as probes is thus conceivable.

Our results reveal that the actual folding of the elongated sequences varies with the nature of the cation present in solution, in stark contrast to non-elongated TBA, which always adopts the antiparallel conformation. For some cations, distinct types of structure are observed for GTAGGT-TBA and TTTTTT-TBA. This shows that the folding into a parallel or an antiparallel quadruplex of the elongated TBA sequences depends not only on the cation, but also on the exact sequence of additional nucleotides. Table 3 provides a summary of the type of intramolecular quadruplex observed for each sequence in the presence of the various studied cations.

Table 3. Dominant type of quadruplex observed for the three oligonucleotides in the presence of all studied cations.

| Cation | TBA | GTAGGT-TBA | TTTTTT-TBA |
|---|---|---|---|
| $Ba^{2+}$ | antiparallel | antiparallel | antiparallel |
| $Ca^{2+}$ | antiparallel | parallel | parallel + antiparallel |
| $K^+$ | antiparallel | antiparallel | antiparallel |
| $Mg^{2+}$ | antiparallel | parallel | parallel + antiparallel |
| $Na^+$ | antiparallel | parallel | parallel + antiparallel |
| $NH_4^+$ | antiparallel | parallel + antiparallel | parallel + antiparallel |
| $Rb^+$ | antiparallel | antiparallel | antiparallel |
| $Sr^{2+}$ | antiparallel | antiparallel | antiparallel |
| $[Ru(NH_3)_6]^{2+}$ | antiparallel | parallel | parallel |
| $[Ru(NH_3)_6]^{3+}$ | antiparallel | parallel | parallel |

The present results have a significant relevance for the development of biosensors based on TBA. For instance, any contact between a biosensor that uses the lengthened sequences as probes and a solution containing $Na^+$, $Ca^{2+}$, $Mg^{2+}$ or $NH_4^+$ can induce the parallel quadruplex folding of all or part of the immobilized probes. This could give rise to the detection of false positives due to the conformational change. Control experiments involving these cations will be necessary to evaluate the performances of such biosensors. It would also be opportune to compare the biosensing results obtained for the lengthened sequences with those of TBA, the apparently cation-insensitive conformation of which decreases the risk of observing false positives. Additionally, the thermal stability of the folded structures, which depends both on the nature of the cations and on the sequence, impacts the choice of the probe sequence that should be adapted with respect to the working temperature range desired for the sensor.

Such careful characterizations are obviously required in the case of electrochemical aptamer-based biosensors. The influence of the frequently used redox marker $[Ru(NH_3)_6]^{3+}$ on the folding of quadruplexes has been studied here for the first time. The ability of this complex ion to promote a parallel quadruplex conformation at very low concentrations is very interesting. In particular, the competition effect shows that the elongated sequences behave as ion-sensitive conformational switches; this opens many perspectives, such as "logic gates" or redox-active responsive devices.

## Experimental Section

Three oligonucleotides were studied; their sequence and molar absorption coefficients at 25 °C are given in Table 1. All three oligonucleotides were synthesized and purified by HPLC by Eurogentec (Belgium) and used without further purification. The lyophilized samples were dissolved to a concentration of 1 mM (per strand) in Tris buffer (10 mM, pH 7.4). Stock solutions were stored at −20 °C and used within one month of their dissolution. All studied samples were prepared by dilution of the stock solution in Tris buffer (10 mM, pH 7.4) to a final concentration that gave an optimal absorbance at 260 nm between 0.7 and 0.8. The exact concentration of each sample was determined by using a Unicam 5626 UV/Vis spectrometer. This concentration was then used to convert all spectra into $\varepsilon$ (UV absorption) or $\Delta\varepsilon$ (CD spectra) according to the Beer–Lambert equation.

The concentration for all monovalent cations was 25 mM, and 5 mM for all divalent cations. Lower hexa-amminеruthenium cation concentrations were used to record the CD spectra because both the oxidized and the reduced form of the complex absorb in the wavelength range of interest (absorption spectra can be found in the Supporting Information). We decided to work with 10 equiv $[Ru(NH_3)_6]^{2+/3+}$ per DNA strand as no more changes were observed in the spectra by further increasing the ruthenium complex concentration.

CD spectra were measured with a Jobin–Yvon Mark VI dichrograph in 1 cm path length quartz Hellma cells at 5 °C except for the temperature denaturation experiments. The temperature-induced melting curves were measured with a UV/Vis spectrometer Varian Cary 4000 (Australia). The temperature was increased/decreased by 1 °C intervals and the samples were equilibrated for 2 min before each measurement.

In UV melting curves, the absorbance was normalized versus its lowest value, $\varepsilon/\varepsilon_{denatured}$. This normalization enabled a comparison based on a common reference point, which is the unfolded state observed at high temperature regardless of the cation present in solution. This normalization procedure avoids the use of the implicit hypothesis that all strands are folded at the lowest measured temperature, and also facilitates the comparison of the amplitudes of the hypochromic shifts. Thermal difference spectra (TDS) were obtained by subtraction of the absorption spectrum of the folded DNA strands from the spectrum of the unfolded DNA strands, $\Delta\varepsilon_{TDS}=\varepsilon_{unfolded}-\varepsilon_{folded}$, according to the convention used by Mergny and co-workers.[29] The temperatures corresponding to folded and unfolded states were chosen as close as possible to each other.

## Acknowledgements

The authors gratefully thank Prof. E. Paleček and Dr. Th. Doneux for fruitful suggestions and discussions. They also acknowledge the Wallonie–Bruxelles International for funding the stays of A.D.R at the Institute of Biophysics of Brnö.

[1] C. Tuerk, L. Gold, *Science* **1990**, *249*, 505–510.
[2] L. C. Bock, L. C. Griffin, J. A. Latham, E. H. Vermaas, J. J. Toole, *Nature* **1992**, *355*, 564–566.
[3] T. Mairal, V. Cengiz Özalp, P. Lozano Sánchez, M. Mir, I. Katakis, C. O'Sullivan, *Anal. Bioanal. Chem.* **2008**, *390*, 989–1007.
[4] a) M. Fialová, J. Kypr, M. Vorlíčková, *Biochem. Biophys. Res. Commun.* **2006**, *344*, 50–54; b) B. I. Kankia, L. A. Marky, *J. Am. Chem. Soc.* **2001**, *123*, 10799–10804; c) J. A. Kelly, J. Feigon, T. O. Yeates, *J. Mol. Biol.* **1996**, *256*, 417–422; d) R. F. Macaya, P. Schultze, F. W. Smith, J. A. Roe, J. Feigon, *Proc. Natl. Acad. Sci. USA* **1993**, *90*, 3745–3749; e) X.-a. Mao, W. H. Gmeiner, *Biophys. Chem.* **2005**, *113*, 155–160; f) S. Nagatoishi, Y. Tanaka, K. Tsumoto, *Biochem. Biophys. Res. Commun.* **2007**, *352*, 812–817; g) I. Smirnov, R. H. Shafer, *J. Mol. Biol.* **2000**, *296*, 1–5.
[5] N. Hamaguchi, A. Ellington, M. Stanton, *Anal. Biochem.* **2001**, *294*, 126–131.
[6] a) V. Ostatná, H. Vaisocherová, J. Homola, T. Hianik, *Anal. Bioanal. Chem.* **2008**, *391*, 1861–1869; b) S. Balamurugan, A. Obubuafo, R. L. McCarley, S. A. Soper, D. A. Spivak, *Anal. Chem.* **2008**, *80*, 9630–9634; c) Q. Tang, X. Su, K. P. Loh, *J. Colloid Interface Sci.* **2007**, *315*, 99–106; d) S. Balamurugan, A. Obubuafo, S. A. Soper, R. L. McCarley, D. A. Spivak, *Langmuir* **2006**, *22*, 6446–6453; e) H. Hasegawa, K.-i. Taira, K. Sode, K. Ikebukuro, *Sensors* **2008**, *8*, 1090–1098.
[7] a) A. Bini, M. Minunni, S. Tombelli, S. Centi, M. Mascini, *Anal. Chem.* **2007**, *79*, 3016–3019; b) T. Hianik, V. Ostatná, M. Sonlajtnerova, I. Grman, *Bioelectrochemistry* **2007**, *70*, 127–133; c) T. Hianik, V. Ostatná, Z. Zajacová, E. Stoikova, G. Evtugyn, *Bioorg. Med. Chem. Lett.* **2005**, *15*, 291–295; d) M. Liss, B. Petersen, H. Wolf, E. Prohaska, *Anal. Chem.* **2002**, *74*, 4488–4495.
[8] B. Basnar, R. Elnathan, I. Willner, *Anal. Chem.* **2006**, *78*, 3638–3642.
[9] X. Wang, J. Zhou, W. Yun, S. Xiao, Z. Chang, P. He, Y. Fang, *Anal. Chim. Acta* **2007**, *598*, 242–248.
[10] a) S. Centi, S. Tombelli, M. Minunni, M. Mascini, *Anal. Chem.* **2007**, *79*, 1466–1473; b) H. Cai, T. M.-H. Lee, I. M. Hsing, *Sensor. Actuat. B-Chem.* **2006**, *114*, 433–437; c) M. Mir, M. Vreeke, I. Katakis, *Electrochem. Commun.* **2006**, *8*, 505–511; d) Y. Xiao, A. A. Lubin, A. J. Heeger, K. W. Plaxco, *Angew. Chem.* **2005**, *117*, 5592–5595; *Angew. Chem. Int. Ed.* **2005**, *44*, 5456–5459; e) Y. Xiao, B. D. Piorek, K. W. Plaxco, A. J. Heeger, *J. Am. Chem. Soc.* **2005**, *127*, 17990–17991; f) J. A. Lee, S. Hwang, J. Kwak, S. I. Park, S. S. Lee, K.-C. Lee, *Sensor. Actuat. B-Chem.* **2008**, *129*, 372–379; g) K. Ikebukuro, C. Kiyohara, K. Sode, *Biosens. Bioelectron.* **2005**, *20*, 2168–2172; h) A.-E. Radi, J. L. Acero Sánchez, E. Baldrich, C. K. O'Sullivan, *Anal. Chem.* **2005**, *77*, 6320–6323.
[11] S. Balamurugan, A. Obubuafo, S. Soper, D. Spivak, *Anal. Bioanal. Chem.* **2008**, *390*, 1009–1021.
[12] a) C. B. Harley, A. B. Futcher, C. W. Greider, *Nature* **1990**, *345*, 458–460; b) N. Kim, M. Piatyszek, K. Prowse, C. Harley, M. West, P. Ho, G. Coviello, W. Wright, S. Weinrich, J. Shay, *Science* **1994**, *266*, 2011–2015.
[13] D. Renciuk, I. Kejnovska, P. Skolakova, K. Bednarova, J. Motlova, M. Vorlickova, *Nucleic Acids Res.* **2009**, *37*, 6625–6634.
[14] I. Smirnov, R. H. Shafer, *Biochemistry* **2000**, *39*, 1462–1468.
[15] a) D. Miyoshi, A. Nakao, T. Toda, N. Sugimoto, *FEBS Lett.* **2001**, *496*, 128–133; b) A.-E. Radi, C. K. O'Sullivan, *Chem. Commun.* **2006**, 3432–3434; c) A. Włodarczyk, P. Grzybowski, A. Patkowski, A. Dobek, *J. Phys. Chem. B* **2005**, *109*, 3594–3605; d) T. Simonsson, *Biol. Chem.* **2001**, *382*, 621–628.
[16] a) T. Li, S. Dong, E. Wang, *Anal. Chem.* **2009**, *81*, 2144–2149; b) D.-L. Ma, D. S.-H. Chan, B. Y.-W. Man, C.-H. Leung, *Chem. Asian J.* **2011**, *6*, 986–1003.
[17] T. Li, E. Wang, S. Dong, *J. Am. Chem. Soc.* **2009**, *131*, 15082–15083.
[18] J. Zhang, Y. Wan, L. Wang, S. Song, D. Li, C. Fan, *Electrochem. Commun.* **2008**, *10*, 1258–1260.
[19] A. L. Dumas, N. W. Luedtke, *J. Am. Chem. Soc.* **2010**, *132*, 18004–18007.

  

[20] D. Monchaud, P. Yang, L. Lacroix, M.-P. Teulade-Fichou, J.-L. Mergny, *Angew. Chem.* **2008**, *120*, 4936–4939; *Angew. Chem. Int. Ed.* **2008**, *47*, 4858–4861.
[21] A. B. Steel, T. M. Herne, M. J. Tarlov, *Anal. Chem.* **1998**, *70*, 4670–4677.
[22] J. Kypr, I. Kejnovska, D. Renciuk, M. Vorlickova, *Nucleic Acids Res.* **2009**, *37*, 1713–1725.
[23] a) T. M. Jovin, D. M. Soumpasis, L. P. McIntosh, *Annu. Rev. Phys. Chem.* **1987**, *38*, 521–560; b) P. S. Ho, C. A. Frederick, D. Saal, A. H. Wang, A. Rich, *J. Biomol. Struct. Dyn.* **1987**, *5*, 521–534.
[24] X. Mao, L. A. Marky, W. H. Gmeiner, *J. Biomol. Struct. Dyn.* **2004**, *22*, 25–33.
[25] C.-F. Tang, R. H. Shafer, *J. Am. Chem. Soc.* **2006**, *128*, 5966–5973.
[26] J.-L. Mergny, A.-T. Phan, L. Lacroix, *FEBS Lett.* **1998**, *435*, 74–78.
[27] J.-L. Mergny, L. Lacroix, *Oligonucleotides* **2003**, *13*, 515–537.
[28] J.-L. Mergny, A. De Cian, A. Ghelab, B. Saccà, L. Lacroix, *Nucleic Acids Res.* **2005**, *33*, 81–94.
[29] J.-L. Mergny, J. Li, L. Lacroix, S. Amrane, J. B. Chaires, *Nucleic Acids Res.* **2005**, *33*, e138.
[30] a) T. Coppola, M. Varra, G. Oliviero, A. Galeone, G. D'Isa, L. Mayol, E. Morelli, M.-R. Bucci, V. Vellecco, G. Cirino, N. Borbone, *Bioorg. Med. Chem.* **2008**, *16*, 8244–8253; b) A. Pasternak, F. J. Hernandez, L. M. Rasmussen, B. Vester, J. Wengel, *Nucleic Acids Res.* **2011**, *39*, 1155–1164.
[31] I. Kejnovská, J. Kypr, M. Vorlícková, *Biochem. Biophys. Res. Commun.* **2007**, *353*, 776–779.

Received: October 27, 2011
Published online: February 23, 2012

  